2008 IEEE International Conference on
Robotics and Automation
Pasadena, CA, USA, May 19-23, 2008

Nonlinear and Geometric Optimization Methods for LADAR Calibration

B. Guerreiro*, C. Silvestre*, P. Oliveira* and J. F. Vasconcelos*
Instituto Superior Técnico, Institute for Systems and Robotics
Av. Rovisco Pais, 1, 1049-001 Lisboa, Portugal
{bguerreiro,cjs,pjcro,jfvasconcelos}@isr.ist.utl.pt

Abstract— **This paper proposes two estimation algorithms for the determination of attitude installation matrix for Laser Detection and Ranging systems (LADAR) mounted onboard autonomous vehicles. The use of autonomous vehicles equipped with LADAR systems to conduct fully automatic surveys of terrain, infrastructures, or just to navigate safely in unknown environments, motivates the research on increasingly precise LADAR data acquisition and processing algorithms, for which the determination of the correct installation matrix is critical. The proposed methods rely on the minimization of the errors between the measured data set and a representation of the real calibration surface. To minimize this error, two nonlinear optimization techniques are proposed, one that estimates the ZYX Euler angles and a second that uses optimization tools for Riemannian manifolds enabling direct estimation of the installation matrix on the group of special orthogonal matrices SO(3). The proposed techniques are extensively tested and their effectiveness compared resorting to simulated LADAR data sets under realistic noise conditions.**

I. INTRODUCTION

Laser Detection and Ranging (LADAR) systems technology is nowadays widely used by the robotics and the remote sensing research communities. The development of airborne laser ranging sensors started in the 1970s in North America, mainly for topographic applications, and later, with the development of affordable Inertial Navigation System (INS) and Global Positioning System (GPS) units, other applications captured the attention of the research community, such as monitoring ice sheets [1] or measuring canopy heights [2]. The robotics research community is nowadays employing autonomous vehicles equipped with LADARs to perform automatic acquisition and 3-D reconstruction of terrain, buildings, large infrastructures or using this information to safely navigate through unknown environments [3], [4]. For all these applications the data accuracy is essential. However, there are several sources of inaccuracy that can lead to considerable nonlinear reconstruction errors, for instance, an airborne LADAR acquiring terrain elevation 1 km above the ground, with 0.01 rad of roll mounting bias will generate points with an error of 10 m, with a planar terrain (otherwise nonlinear distortions will appear). Thus, the calibration of these errors, specially the attitude installation bias, is fundamental to achieve the desired accuracy requirements.

In most applications the LADAR system is installed in a platform equipped with an INS/GPS unit, which provides position and attitude data that together with the relative distance measured by the LADAR enables the reconstruction of the surrounding environment. Conversely to other calibration problems, the available information for LADAR calibration is only clouds of 3-D points, with no matching information between them, and most calibration procedures require particular terrain features, and specific vehicle trajectories in order to calibrate a subset of the parameters [5]. For instance, flying over a flat surface while performing pitch and roll maneuvers, separately, enables the calibration of only these two parameters. Since there is no direct technique to compare the measured data set with the corresponding real points, the idea is to compare the measured data set with a representation of the real surface [6]. This technique is used in [7] with the linearization of the error model to obtain a Gauss-Helmert model, used then to estimate the installation bias.

The estimation problem is formulated within the scope of maximum likelihood (ML) theory [8] allowing the formulation of the calibration problem as an optimization problem defined by the minimization of the errors between the measured data set and the real surface, yielding a weighted scalar cost function, for which two different minimization techniques are proposed. The first technique consists of estimating the ZYX Euler angles that parameterize the installation offset rotation matrix. This approach uses basic concepts of nonlinear optimization, like the Gradient and Newton methods to find a search direction, as well as line search algorithms, like the Wolfe rule, to compute the step size [9], [10]. The second approach resorts to optimization tools on Riemannian manifolds enabling the use of Gradient and Newton methods to directly estimate the installation matrix on the group of special orthogonal matrices SO(3) [11], [12]. This approach can also use the Wolfe rule to compute the step size, nonetheless, there exists an exact computation of the step size improving the performance of the algorithm [13]. The proposed calibration techniques are compared using simulated data sets to assess their performance and limitations in the presence of noise.

The paper is organized as follows: Section II introduces the reconstruction error model, a ML formulation is proposed, and the calibration problem is written as a nonlinear

*This work was partially supported by Fundação para a Ciência e a Tecnologia (ISR/IST pluriannual funding) and project MEDIRES from ADI through the POS Conhecimento Program that includes FEDER funds, and by the project PTDC/EEA-ACR/72853/2006 HELICIM project. The work of Bruno Guerreiro and José Vasconcelos was supported by the PhD Student Grants SFRH/BD/18954/2004 and SFRH/BD/21781/2005, respectively, from the Portuguese FCT POCTI programme.

978-1-4244-1647-9/08/$25.00 ©2008 IEEE.

optimization problem. In Section III the optimization problem is addressed using ZYX Euler angles and section IV introduces Riemannian optimization tools. Simulation results and an in depth comparison of the different algorithms are presented in Section V. Finally, in Section VI the main conclusions are offered and directions for further work are outlined.

II. Reconstruction Error Model

In this section the reconstruction error model and the calibration problem are introduced. The reconstruction error is generated by the computation of the 3-D points using the measured range and angle provided by the LADAR, assuming that the calibration parameters are correct. The calibration problem is to find the optimal calibration parameters that minimize the error between the set of reconstructed points, $\mathcal{P}_m$, and the real surface $\mathcal{S}_{\text{real}}$. The measured set of points $\mathcal{P}_m = \{\mathbf{p}_i\}$, $i = 1, \ldots, n_m$, where n_m is the number of measured reconstructed points. In the following three subsections, the point reconstruction, the point-surface comparison and the calibration problem are introduced.

A. Point Reconstruction

The point reconstruction model describes the transformation of the LADAR raw data, composed by a range measurement and an incidence angle, into 3-D points. The following coordinate frames are introduced: $\{I\}$ as the inertial frame; $\{ins\}$ as INS/GPS frame; $\{l\}$ as the LADAR frame, with origin at the laser's firing point and z-axis indicating the zero scanning angle; $\{lb\}$ as the laser beam frame, with origin at the firing point, y-axis collinear with that of frame $\{l\}$ and z-axis oriented opposite to the direction of the laser beam. These frames and the connections between them are depicted in Fig. 1. Each measurement i is defined as the distance

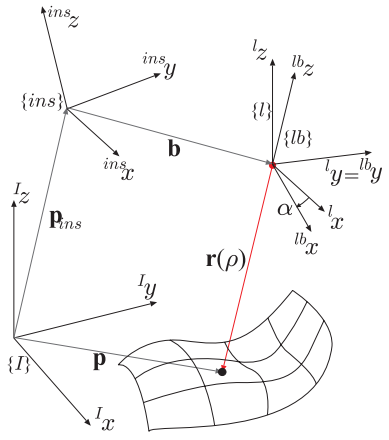

Fig. 1. Ladar coordinate frames

between the laser firing point and the laser hit point, ρ_i, and by the angular position of the laser beam, α_i, that is, the angle from $\{l\}$ to $\{lb\}$. Thus, it can easily be seen that the expression that transforms the LADAR measurement (ρ_i, α_i) into the reconstructed 3-D point $\mathbf{p}_i$, expressed in the inertial frame, is given by

$$\mathbf{p}_i = R_{ins_i} \left(R\, R_l\, R_{lb}(\alpha_i)\, \mathbf{r}(\rho_i) + \mathbf{b} \right) + \mathbf{p}_{ins_i} \ , \qquad (1)$$

where R_{ins_i} is the platform attitude defined by the rotation from $\{ins\}$ to $\{I\}$, R_l is the known attitude mounting bias defined by the rotation from $\{l\}$ to $\{ins\}$, $R_{lb}(\alpha_i)$ is the rotation from $\{lb\}$ to $\{l\}$, that defines the laser beam rotation and is given by $R_{lb}(\alpha_i) = R_Y(\alpha_i)$, with $R_Y(.)$ standing for the rotation matrix about the y axis, $\mathbf{r}(\rho_i) = \begin{bmatrix} 0 & 0 & -\rho_i \end{bmatrix}'$, $\mathbf{p}_{ins_i}$ is the INS/GPS unit position expressed in $\{I\}$. The known position installation bias $\mathbf{b}$ denotes the laser firing point described in $\{ins\}$ and matrix R is the rotation matrix that defines the unknown attitude installation bias, which is an element of the group of special orthogonal matrices SO(3). Let $\mathrm{M}(n, \mathbb{R}) = \{A : n \times n \text{ matrix with real entries}\}$ and the group of orthogonal matrices be defined as $\mathrm{O}(n) = \{U \in \mathrm{M}(n, \mathbb{R}) : U\,U' = I_{n \times n}\}$, then the group of special ortogonal matrices is $\mathrm{SO}(n) = \{R \in \mathrm{O}(n) : \det(R) = 1\}$.

B. Point-Surface Comparison

The fact that in this problem there is no correspondence between the points of the real surface $\mathcal{S}_{\text{real}}$ and the measurement set $\mathcal{P}_m$, does not alow for a direct comparison. The proposed solution consists of comparing $\mathcal{P}_m$ with an approximation of the real surface, $\mathcal{S}_{\text{approx}}$. Therefore, the following assumptions are considered:

Assumption 1 (Elevation map): The real surface $\mathcal{S}_{\text{real}}$ can be approximated by an elevation map, i. e., the height of the surface can be expressed as a function $f_{\mathcal{S}} : \mathbb{R}^2 \rightarrow \mathbb{R}$ of the x and y coordinates, $z = f_{\mathcal{S}}(x, y)$.

Assumption 2 (Set of planes): The surface $\mathcal{S}_{\text{real}}$ can be approximated by a piecewise surface $\mathcal{S}_{\text{approx}}$ defined by a set of n_p planes, with arbitrarily small error (as $n_p \rightarrow \infty$).

To compare the points $\mathbf{p}_i \in \mathcal{P}_m$ with the surface $\mathcal{S}_{\text{approx}}$, each point is linked with the closest plane along its normal vector. Considering the set of planes that define $\mathcal{S}_{\text{approx}}$, let plane i be defined by the plane equation $\mathbf{s}_i'\,\mathbf{p}_i + s_i^4 = 0$, where $\mathbf{s}_i = \begin{bmatrix} s_i^1 & s_i^2 & s_i^3 \end{bmatrix}' \in \mathbb{R}^3$ is the i-th plane normal unitary vector and $s_i^4 \in \mathbb{R}$.

C. Calibration Problem

The calibration of a LADAR system can be formulated as the minimization of the error between the measured set of reconstructed points $\mathcal{P}_m$ and the surface $\mathcal{S}_{\text{approx}}$, subject to the LADAR model constraint. The error between each point $\mathbf{p}_i$ and the associated plane of the control surface can be defined as $\mathbf{e}_i = \mathbf{p}_{0_i} - \mathbf{p}_i$ where $\mathbf{p}_{0_i} = \mathbf{p}_i - \mathbf{s}_i\, D_i$ denotes the point in the plane closest to $\mathbf{p}_i$ and $D_i = \mathbf{s}_i'\,\mathbf{p}_i + s_i^4$ is the distance along $\mathbf{s}_i$ between $\mathbf{p}_i$ and $\mathbf{p}_{0_i}$. Hence, after some algebraic manipulation, the measurement error expression can be written as

$$\mathbf{e}_i(R) = H_i\, R\, \mathbf{h}_i + \mathbf{c}_i \ , \qquad (2)$$

where $H_i = \rho_i\, S_i\, R_{ins_i}$, $\mathbf{h}_i = -R_l\, R_{lb}(\alpha_i)\, \mathbf{r}(1)$, $\mathbf{c}_i = -S_i\, R_{ins_i}\, \mathbf{b} - S_i\, \mathbf{p}_{ins_i} - s_i^4\, \mathbf{s}_i$ and $S_i = \mathbf{s}_i\, \mathbf{s}_i'$. Also, $R \in \mathrm{SO}(3)$ is the calibration parameter matrix to be estimated and the known parameters are $H_i \in \mathrm{M}(3, \mathbb{R})$ and $\mathbf{h}_i, \mathbf{c}_i \in$

$\mathbb{R}^3$. In addition, the following assumption characterizes the measurement error distribution.

Assumption 3 (Error distribution): The measurement error distribution is assumed to be Gaussian and defined by $p(\mathbf{e}_i) = \mathcal{N}\left(\mathbf{e}_i; \mathbf{0}, \sigma_i^2\, I\right)$.

The calibration problem can be formulated within the scope of the ML estimation theory as that of maximizing the reconstruction error probability function, i. e.

$$R^* = \arg\min_R f(R) \quad , \quad \text{s. t.} \quad R \in \text{SO(3)}\,, \tag{3}$$

with $f(R) = \sum_{i=1}^{n} \frac{1}{2\,\sigma_i^2}\, \|\mathbf{e}_i(R)\|^2$. The usage of the following nonlinear optimization techniques with Newton method, instead of standard nonlinear least squares methods, allows for a more efficient estimation algorithm, since the second order derivative of the cost functional is used.

III. Optimization on Euler Angles Space

In this section the optimization problem is reformulated to estimate the angle vector, $\mathbf{x}$, instead of the rotation matrix R. Let $\mathbf{x} \in \mathbb{R}^3$ be the ZYX Euler angles representation of the rotation matrix, i. e. $R = R(\mathbf{x})$, then, the optimization problem (3) can be written as

$$\mathbf{x}^* = \arg\min_{\mathbf{x}}\ f(\mathbf{x}) \tag{4}$$

with $f : \mathbb{R}^3 \to \mathbb{R}$ given by

$$f(\mathbf{x}) \quad = \quad \sum_{i=1}^{n} \frac{1}{2\,\sigma_i^2}\, \|H_i\, R(\mathbf{x})\, \mathbf{h}_i + \mathbf{c}_i\|^2 \ . \tag{5}$$

The estimated calibration parameters, denoted by $\hat{\mathbf{x}}$, are computed using the Gradient and Newton methods, that at each k iteration provide a descent direction, $\mathbf{d}_k \in \mathbb{R}^6$. This descent direction is used to update the next estimate $\mathbf{x}_{k+1}$ by solving a minimization subproblem, usually called line search, to find the optimal step size along the direction $\mathbf{d}_k$. This is formalized in Algorithm 1, where $\gamma_{\mathbf{d}_k}(t) = \mathbf{x}_k + t\,\mathbf{d}_k$.

Algorithm 1: Minimization algorithm for the LADAR calibration problem:

1) Initialize $\mathbf{x}_0$ and let k = 0;
2) Compute descent direction $\mathbf{d}_k$;
3) Compute the step size by solving the minimization subproblem $t_k^* = \arg\min_{t \geq 0} f\left(\gamma_{\mathbf{d}_k}(t)\right)$;
4) Compute next parameter estimate: $\mathbf{x}_{k+1} = \gamma_{\mathbf{d}_k}(t_k^*)$;
5) Test if $\left\|\nabla f|_{\mathbf{x}_{k+1}}\right\| < \epsilon$: if true, let $\hat{\mathbf{x}} = \mathbf{x}_{k+1}$ be the final estimated parameter and stop; if false, let $k \leftarrow k+1$ and go to step 2.

A. Descent Direction

To compute the descent direction $\mathbf{d}_k$, the most widely used method is the Gradient method, for which $\mathbf{d}_k$ is computed using the gradient of the cost functional, $\nabla f(\mathbf{x})|_{\mathbf{x}}$. The Newton method uses the Hessian matrix, denoted by $\nabla^2 f(\mathbf{x})|_{\mathbf{x}}$, yielding faster convergence near the optimum value.

The descent direction for the gradient method is given by

$$\mathbf{d}_k = -\nabla f(\mathbf{x})|_{\mathbf{x}} \tag{6}$$

where the gradient is computed using

$$\nabla f(\mathbf{x})|_{\mathbf{x}} = \left[\ \frac{\partial\, f(\mathbf{x})}{\partial x_1} \quad \frac{\partial\, f(\mathbf{x})}{\partial x_2} \quad \frac{\partial\, f(\mathbf{x})}{\partial x_3}\ \right]' , \tag{7}$$

$$\frac{\partial\, f(\mathbf{x})}{\partial x_j} = \sum_{i=1}^{n} \frac{1}{\sigma_i^2}\, \mathbf{e}_i'\, H_i\, \frac{\partial\, R(\mathbf{x})}{\partial x_j}\, \mathbf{h}_i \ . \tag{8}$$

For the Newton method, the descent direction is defined by

$$\mathbf{d}_k = -\left(\nabla^2 f(\mathbf{x})|_{\mathbf{x}}\right)^{-1}\, \nabla f(\mathbf{x})|_{\mathbf{x}} \tag{9}$$

where Hessian matrix is given by

$$\nabla^2 f(\mathbf{x})|_{\mathbf{x}} = \frac{\partial^2\, f(\mathbf{x})}{\partial \mathbf{x}\, \partial \mathbf{x}'} = \left\{ \frac{\partial^2 f}{\partial x_j\, \partial x_l} \right\}, \tag{10}$$

$$\begin{aligned} \frac{\partial^2 f}{\partial x_j\, \partial x_l} = \sum_{i=1}^{n} \frac{1}{\sigma_i^2} \Bigg[& \mathbf{e}_i'\, H_i\, \frac{\partial^2\, R(\mathbf{x})}{\partial x_j\, \partial x_l}\, \mathbf{h}_i + \\ & + \left(H_i\, \frac{\partial\, R(\mathbf{x})}{\partial x_j}\, \mathbf{h}_i \right)' \left(H_i\, \frac{\partial\, R(\mathbf{x})}{\partial x_l}\, \mathbf{h}_i \right) \Bigg] . \end{aligned} \tag{11}$$

B. Line Search

The step size optimization subproblem in Algorithm 1 is numerically solved using the Wolfe conditions [10]. Consider the function $\phi : \mathbb{R} \to \mathbb{R}$ defined by $\phi(t) = f\left(\mathbf{x}_k + t\,\mathbf{d}_k\right)$ and derivative given by $\dot{\phi}(t) = \nabla' f|_{\mathbf{x}_k + t\,\mathbf{d}_k}\, \mathbf{d}_k$ and let also $\mu_k = \phi(0) + \sigma\, \dot{\phi}(0)\, t_k$ and $\mu_0 = \lambda\, \dot{\phi}(0)$, where σ and λ are parameters of the algorithm. The Wolfe rule classifies the step size according to the sets

$$\begin{aligned} \mathcal{A} &= \left\{ t_k > 0 : \phi(t_k) \leq \mu_k \ \wedge\ \dot{\phi}(t_k) \geq \mu_0 \right\} \\ \mathcal{D} &= \left\{ t_k > 0 : \phi(t_k) > \mu_k \right\} \\ \mathcal{E} &= \left\{ t_k > 0 : \phi(t_k) \leq \mu_k \ \wedge\ \dot{\phi}(t_k) < \mu_0 \right\} \end{aligned} \tag{12}$$

that define the acceptable, the right unacceptable and the left unacceptable step sizes, respectively. The line search algorithm consists of finding an acceptable step size, i. e., an estimate of the optimal step size.

IV. Optimization on Riemannian Manifolds

This section introduces the optimization methodology on Riemannian manifolds. Since the rotation matrix R is an element of the group of special orthogonal matrices SO(3) which is an embedded submanifold of $M(3, \mathbb{R})$, the optimization tools adopted in this section are based on simple exercises of Riemannian Geometry theory and allow for the minimization of the likelihood function directly on the manifold of special orthogonal matrices SO(3). The concepts of intrinsic gradient and Hessian derived for SO(3) produce descent directions in the manifold and the cost functional is minimized along geodesics in SO(3). For a comprehensive introduction to the subject and for applications with orthogonality constraints the reader is referred to [11], [12].

Considering the log-likelihood function $f : \text{SO(3)} \to \mathbb{R}$ given by

$$f(R) \quad = \quad \sum_{i=1}^{n} \frac{1}{2\,\sigma_i^2}\, \|H_i\, R\, \mathbf{h}_i + \mathbf{c}_i\|^2 \ , \tag{13}$$

the optimization problem reduces to the one defined in (3). The estimate $\hat{R}$ of the optimal value R^* is computed using the Gradient or the Newton methods generalized to manifolds. Given the current parameter estimate R_k at iteration k, these methods compute a descent direction in the intrinsic tangent space, $\mathbf{d}_k \in T_{R_k}\text{SO(3)}$, and obtain the new estimate R_{k+1} by solving a minimization subproblem along the geodesic of the manifold. This algorithm is structured as Algorithm 1, however, $\gamma_{\mathbf{d}_k}(t) \in \text{SO(3)}$ is defined as the geodesic of the manifold with initial conditions $\gamma_{\mathbf{d}_k}(0) = R_k$ and $\dot{\gamma}_{\mathbf{d}_k}(0) = \mathbf{d}_k$.

The accuracy of the estimate is determined by the constant ϵ and the norm is determined using the metrics in the parameter space SO(3). Hence it is necessary to define the metric for the rotation matrix $R \in \text{SO(3)}$, which is inherited from the canonical metric in the Euclidean space M(3,$\mathbb{R}$). While the tangent space of M(3,$\mathbb{R}$) is identified with $T_R\text{M(3,}\mathbb{R}) \simeq \text{M(3,}\mathbb{R})$ and represented by the usual gradient, the tangent space of SO(3) at point R is identified by $T_R\text{SO(3)} \simeq R\text{K(3)} = \{R\,K : K \in \text{K(3)}\}$, where $\text{K}(n) = \{K \in \text{M}(n,\mathbb{R}) : K = -K'\}$. To define the canonical metric in SO(3), let two tangent vectors $\{\delta_1, \delta_2\} \in T_R\text{SO(3)}$, which are identified by $\delta_1 \simeq R\,K_1$ and $\delta_2 \simeq R\,K_2$, with $\{K_1, K_2\} \in \text{K(3)}$, then $\langle \delta_1, \delta_2 \rangle = \text{tr}\,(\delta_1'\,\delta_2)$, where tr (.) stands for the trace of a matrix.

The following three sections address: a) the computation of a descent direction, using both the gradient and the Newton methods, b) the line search algorithm with Wolfe conditions and c) the deterministic line search algorithm that computes an exact step size.

A. Descent Direction

To improve the accuracy of the descent direction estimate, a generalization for manifolds of the Gradient and the Newton methods is adopted. While the former is easier to derive and implement, the Newton method yields very fast convergence near the minimum. The derivation of the gradient and the Hessian of the log-likelihood function are described below specifically for the SO(3) manifold.

1) Gradient Method: The log-likelihood function (13) can be generalized to M(3,$\mathbb{R}$) by defining the smooth function $\hat{f} : \text{M(3,}\mathbb{R}) \rightarrow \mathbb{R}$ such that $\hat{f}|_{\text{SO(3)}} = f$. The tangent space on M(3,$\mathbb{R}$) is characterized as the direct sum of two tangent spaces complementary to SO(3), that is

$$T_R\text{M(3,}\mathbb{R}) = T_R\text{SO(3)} \oplus (T_R\text{SO(3)})^{\perp} \ , \qquad (14)$$

where the operator $\oplus$ stands for the direct sum of two sets and $(T_R\text{SO(3)})^{\perp}$ is the orthogonal complement of T_RSO(3). The smooth vector field defined by the extrinsic gradient $\text{grad}\hat{f}|_R \in T_R\text{M(3,}\mathbb{R})$ is decomposed as the sum of its tangent and orthogonal components

$$\text{grad}\hat{f}|_R = \left(\text{grad}\hat{f}|_R\right)^{\top} + \left(\text{grad}\hat{f}|_R\right)^{\perp} \qquad (15)$$

and is identified with the usual gradient in M(3,$\mathbb{R}$), that is

$$\text{grad}\hat{f}|_R \simeq \nabla\hat{f}|_R := \frac{\partial\, f}{\partial R} := \left[\frac{\partial\, f}{\partial r_{ij}}\right]_{i,j\in\{1,2,3\}} . \qquad (16)$$

Hence, the intrinsic gradient $\nabla f|_R \in RK(3)$ is obtained by the projection of the extrinsic gradient on the tangent space T_RSO(3), i.e. $\nabla f|_R = (\nabla\hat{f}|_R)^{\top}$.

The projection of the extrinsic gradient results from an optimization problem with closed solution given by

$$\begin{aligned} \nabla f|_R &= R \arg\min_{K\in\mathcal{K}} \left\| \nabla\hat{f}|_R - R\,K \right\|^2 \\ &= R\,\text{skew}\left(R'\,\nabla\hat{f}|_R\right) \ , \end{aligned} \qquad (17)$$

where $\text{skew}(A) = 1/2\,(A - A')$ is the skew symmetric component of A. The extrinsic gradient expression for the considered cost functional is given by

$$\nabla\hat{f}|_R = \sum_{i=1}^{n} \frac{1}{\sigma_i^2} H_i'\,(H_i\,R\,\mathbf{h}_i + \mathbf{c}_i)\,\mathbf{h}_i' \ . \qquad (18)$$

Thus, at each iteration k the intrinsic gradient direction used in the optimization algorithm is $\mathbf{d}_k = -\nabla f|_R$.

2) Newton Method: The Newton method uses the second order properties of the log-likelihood function to compute descent direction. Although this method is harder to compute and requires more memory, the convergence rate is greater near the optimal value than that of the gradient method.

Given two tangent vectors $\{X, Y\} \in T_R\text{SO(3)}$ and the correspondent extension $\{\hat{X}, \hat{Y}\} \in T_R\text{M(3,}\mathbb{R})$, the intrinsic Hessian is given by compensating the external Hessian

$$\text{Hess}f\,(X,Y) = \text{Hess}\hat{f}\left(\hat{X},\hat{Y}\right) + \Pi_R\,(X,Y)\,\hat{f} \ , \qquad (19)$$

where the second fundamental form $\Pi_R\,(X,Y) : T_R\text{SO(3)} \times T_R\text{SO(3)} \rightarrow (T_R\text{SO(3)})^{\perp}$ is a differentiable local vector field on M(3,$\mathbb{R}$) normal to SO(3). The external Hessian is identified by the usual second order derivative in Euclidean spaces

$$\begin{aligned} \text{Hess}\hat{f}\left(\hat{X},\hat{Y}\right) &= \text{vec}\,(\mathbf{X})'\ \nabla^2\hat{f}|_R\,\text{vec}\,(\mathbf{Y}) \ , \qquad (20) \\ \nabla^2\hat{f}|_R &= \frac{\partial^2\,\hat{f}}{\partial\text{vec}\,(R)\ \partial\text{vec}\,(R)'} \ , \qquad (21) \end{aligned}$$

where $\hat{X} \simeq \mathbf{X} \in \text{M(3,}\mathbb{R})$, $\hat{Y} \simeq \mathbf{Y} \in \text{M(3,}\mathbb{R})$ and the vec (.) operator is the vectorization of a matrix. The second fundamental form applied to $\hat{f}$ yields

$$\Pi_R\,(X,Y)\,\hat{f} = -\langle R\,\text{symm}(X'\,Y), \nabla\hat{f}|_R\rangle \ , \qquad (22)$$

where $\text{symm}(A) = 1/2\,(A + A')$ is the symmetric component of A, and

$$\nabla^2\hat{f}|_R = \sum_{i=1}^{n} \frac{1}{\sigma_i^2} \mathbf{h}_i\,\mathbf{h}_i' \otimes H_i'\,H_i \ , \qquad (23)$$

where $\otimes$ is the Kronecker product operator. The Newton method search direction is the unique tangent vector $\mathbf{d} \in T_R\text{SO(3)}$ that satisfies $\text{Hess}f\,(X,\mathbf{d}) = -\langle X, \mathbf{d}\rangle$ for all $X \in T_R\text{SO(3)}$. Let $\varepsilon = \{\mathbf{E}_1, \mathbf{E}_2, \ldots, \mathbf{E}_m\}$ be an orthonormal basis for T_RSO(3), then the Newton direction coordinates z_i in the basis ε, $\mathbf{d} = \sum_{i=1}^{m} z_i\,\mathbf{E}_i$, are computed by solving the linear system $A_{hess}\,\mathbf{z} = \mathbf{b}_{hess}$, where $A_{hess} = \{\text{Hess}f\,(\mathbf{E}_i, \mathbf{E}_j)\}$, $\mathbf{z} = \{z_j\}$ and $\mathbf{b}_{hess} = -\{\langle \mathbf{E}_i, \nabla f|_R\rangle\}$, for $i, j = 1, \ldots, m$.

B. Line Search

The geodesic is defined as the curve in the manifold with zero acceleration. A geodesic curve is fully characterized by the initial position and velocity conditions, $\gamma_d(0)$ and $\dot{\gamma}_d(0)$ respectively, and to the particular case of SO(3), the geodesic $\gamma_d : J \rightarrow \text{SO(3)}$ is defined as $\gamma_d(t) = R\, e^{R'\,\mathbf{d}\,t}$, where J is an interval in $\mathbb{R}$ and $\mathbf{d} \in RK(3)$ identifies the tangent vector.

As in the approach of Section III, the step size optimization subproblem of Algorithm 1 is numerically solved using the Wolfe conditions, generalized to line search on geodesics. Considering the function $\phi : \mathbb{R} \rightarrow \mathbb{R}$ defined as $\phi(t) = f(\gamma_d(t))$ with derivative given by $\dot{\phi}(t) = \nabla' f|_{\gamma_d(t)}\, \dot{\gamma}_d(t)$ we can introduce the same sets as in (12) and use the same algorithm to provide an estimate of the optimal step size.

C. Deterministic Line Search

Taking advantage of the periodicity of the objective function, the exact optimal solution for line search problem can be found by simply determining the roots of a fourth order polynomial. This can be seen in [13], where this approach is used for a similar cost functional. Given a search direction $\mathbf{d}$, computed using either the Gradient or the Newton methods, the line search optimization subproblem is defined by $t^* = \arg\min_{t \geq 0} \phi(t)$, where $\phi(t) = f(\gamma_d(t))$. To tackle a more general type of optimization problem let the cost functional be written as

$$\begin{aligned} \phi(t) \;\; = \;\; & \sum_{i=1}^{n} \frac{1}{2\,\sigma_i^2} \operatorname{tr}\big(M_i'\, e^{-\Omega\, t}\, R'\, N_i\, R\, e^{\Omega\, t}\, M_i \\ & + 2\, W_i'\, R\, e^{\Omega\, t}\, M_i + C_i\big) \end{aligned} \tag{24}$$

where $M_i = \mathbf{h}_i$, $N_i = H_i' H_i$, $W_i = \mathbf{c}_i' H_i$, $C_i = \mathbf{c}_i' \mathbf{c}_i$ and $\Omega = \frac{1}{\|\boldsymbol{\omega}\|}[\boldsymbol{\omega}\times]$ with $[\boldsymbol{\omega}\times] = R'\,\mathbf{d}$. The skew-symmetric matrix $[\mathbf{a}\times]$ stands for the cross product operator for vector $\mathbf{a}$. In this way Ω has unit length allowing the usage of Rodrigues' formula $e^{\Omega\, t} = I + \Omega \sin t + \Omega^2 (1 - \cos t)$. Substituting this formula into (24) and simplifying, it can be seen that $\phi(t) = k_1 + k_2 \sin t + k_3 \cos t + k_4 \sin 2\,t + k_5 \cos 2\,t$, where k_j, $j = 1, \ldots, 5$ are constant scalars. To find the optimal value for the step size the first order condition of optimality, that is $\frac{d\,\phi(t)}{dt} = 0$, yields $k_2 \cos t - k_3 \sin t + 2\,k_4 \cos 2\,t - 2\,k_5 \sin 2\,t = 0$ and the optimization subproblem is now to find the values of $t \in [0, 2\,\pi[$ for which the previous condition is satisfied.

The first step is to make a trigonometric half-angle substitution, i. e., $x = \tan \frac{t}{2}$, reducing the first order condition of optimality to a fourth order polynomial in x, $x^4 + b_3\, x^3 + b_2\, x^2 + b_1\, x + b_0 = 0$, where b_i, $i = 0, \ldots, 3$ are constant scalars. After finding the roots of this quartic polynomial, which is a standard procedure [14], the optimal value of t is the real root for which the cost functional is minimal.

V. Simulation Results

To compare the performance of the algorithms presented above a digital elevation map is used to define the simulated real surface $\mathcal{S}_{\text{real}}$ and, for the sake of simplicity, the approximated surface $\mathcal{S}_{\text{approx}}$ has lower resolution. This can be seen in the example of the calibration setup shown in Fig. 2, where the platform trajectory (in magenta), the optimal acquired points (in green) and the reconstructed points using the initial condition (in yellow), are overlayed on the approximated surface.

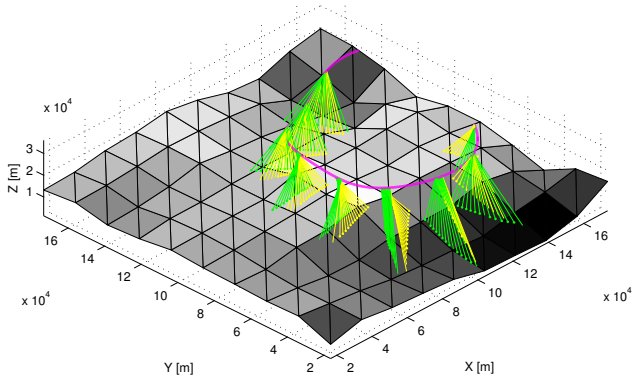

Fig. 2. Calibration example: $\mathcal{S}_{\text{approx}}$, trajectory and laser beams

From the presented optimization methods and line search algorithms, three different configurations are tested: 1) optimization on Euler angles space with Wolfe rule; 2) Riemannian optimization with Wolfe rule; and 3) Riemannian optimization using exact step size. These methods will be compared in this section in order to highlight the advantages and disadvantages of each of them. In all these methods, the computation of the search direction is performed using the Newton's method. Evaluating the Euler angles solution $\mathbf{x}$ as $R(\hat{\mathbf{x}}) \in \text{SO(3)}$, an error distance that is defined in SO(3) is used to compare the solutions of the different configurations. Let $R^*, \hat{R} \in \text{SO(3)}$ be optimal and the estimated rotation matrices, respectively, and let also $\tilde{R} = \hat{R}'\, R^* \in \text{SO(3)}$ be the error matrix, the performance of each method is evaluated by defining the distance from $\tilde{R}$ to I as

$$\|\tilde{R}\|_{\text{SO(3)}} = \arccos\left(\tfrac{1}{2}(\operatorname{tr}(\hat{R}'\, R^*) - 1)\right) .$$

The three methods where tested using a perfectly acquired data set where the acquired points, $\mathcal{P}_m$, belong to the control surface $\mathcal{S}_{\text{approx}}$, and another data set with additive white gaussian noise with zero mean and standard deviation $\sigma = 10^3$ m. The objective is to see the influence of the imperfections when the real surface $\mathcal{S}_{\text{real}}$ is approximated by the control surface $\mathcal{S}_{\text{approx}}$ and also when the acquired points do not belong to the real surface.

The experience consisted of 500 Monte Carlo runs with random initial conditions, and for each initial condition all methods were tested with and without noise addition. The initial conditions were computed using a uniform distribution between $-\frac{\pi}{6}$ and $\frac{\pi}{6}$ for each component of the ZYX Euler angle vector $\mathbf{x}_0$ yielding the rotation matrix $R_0 = R(\mathbf{x}_0)$. The optimal value for all the trials is defined by the rotation matrix, $R^* = R(\mathbf{x}^*)$, obtained from the ZYX Euler angles $\mathbf{x}^* = \begin{bmatrix} 0.10 & 0.05 & -0.04 \end{bmatrix}'$. The stopping criterion used was $\frac{\|\nabla f|_R\|}{\|\nabla f|_{R_0}\|} < 10^{-10}$. All the simulations were performed

TABLE I

SUMMARY OF RESULTS.

		Method		
		1	2	3
Average Computation Time [s]	No Noise	18.1	18.7	14.7
	Noise	30.3	34.8	17.1
Number of Iterations	No Noise	6.8	6.8	5.8
	Noise	7.4	7.9	6.8
Failure [%]	No Noise	5.6	3.0	0
	Noise	5.6	1.4	0
Distance to optimal [rad]	Mean	0.028	0.019	0.016
	Maximum	0.085	0.028	0.023
	Minimum	0.015	0.007	0.016

using Matlab on an Intel Pentium Centrino processor at 1.7 GHz.

Table I presents three statistical indicators of the simulation described above: the average computation time, the number of iterations and the percentage of failure. The first and the second indicators show the efficiency of each method, and it is evident that the Riemannian method with exact step size (method 3) is the best. The percentage of failure is not commonly used, but is justified by the fact that the problem that is being dealt with is nonconvex, since the control surface has discontinuities and even the real surface may introduce local minima. As it can be seen the only method unaffected by this particularities is the one that utilizes the exact step size (method 3). As expected, the Euler and the Riemannian methods, both with Wolfe rule line search, have similar computation times and number of iterations, nevertheless, the Riemannian approach tends to be more reliable on finding the right solution.

To effectively evaluate the performance of each method, the table also presents the average, maximum and minimum distance in SO(3) to the optimal solution with noise addition for each of the methods. Without noise, the maximum error distance for all the methods is less than $5.5 \times 10^{-8}\ [rad]$. In the simulation with noise, as expected, the best performance is obtained with the Riemannian method with exact step size (method 3), followed by the Riemannian method with Wolfe rule (method 2) and finally the Euler method with Wolfe rule (method 1).

Looking at these results we can say clearly that the best of these three methods is the Riemannian optimization using the exact step size, since it consistently presents the best qualities in the analyzed aspects: computation time, number of iterations, no failures and best estimates in the presence of noise.

VI. CONCLUSIONS

This paper deals with the problem of laser calibration by suggesting three numerical optimization methods that estimate the mounting bias rotation matrix $R \in$ SO(3) by minimizing the distances between the acquired laser points and a known control surface. The first method estimating the mounting bias ZYX Euler angle vector, and it was tested using the Newton's method with the Wolfe rule. The second method uses the generalization of the Newton method to SO(3), estimating the mounting bias rotation matrix. To compute the step size it also uses the Wolfe rule as the previous method. Finally, the third method uses the Newton method for SO(3) with an exact computation of the optimal step size instead of the Wolfe rule for the line search algorithm.

The performance and limitations of each of these methods was extensively tested in Matlab and the results indicate that all methods are able to find good estimates for the laser calibration problem. Moreover, the third method displays immunity to local minima, the smallest average estimation error in the presence of noise and the fastest average computation time.

The principal limitation of these methods is introduced by the necessity of a known control surface. One direction of research is to consider scanning trajectories that overlap and minimize the error between the overlapped clouds of data points. Further work is also needed in order to include other sources of reconstruction errors, like the time delay between laser acquisition and the INS/GPS data or the range measurement error.

REFERENCES

[1] W. B. Krabill, R. H. Thomas, C. F. Martin, R. N. Swift, and E. B. Frederick, "Accuracy of airborne laser altimetry over the greenland ice sheet," *International Journal of Remote Sensing*, vol. 16, no. 7, pp. 1211–1222, 1995.

[2] E. Næsset and T. Økland, "Estimating tree height and tree crown properties using airborne scanning laser in a boreal nature reserve," *Remote Sensing of Environment*, vol. 79, no. 1, pp. 105–115, January 2002.

[3] S. Thrun, M. Diel, and D. Hähnel, "Scan alignment and 3-d surface modeling with a helicopter platform," in *Proceedings of the 4th International Conference on Field and Service Robotics*, July 2003.

[4] R. Madhavan and E. Messina, "Iterative registration of 3d ladar data for autonomous navigation," in *Intelligent Vehicles Symposium, 2003. Proceedings.* IEEE, June 2003, pp. 186–191.

[5] J. R. Ridgway, J. Minster, N. Williams, J. L. Bufton, and W. B. Krabill, "Airborne laser altimeter survey of long valley, california," *Geophysical Journal International*, vol. 131, no. 2, pp. 267–280, November 1997.

[6] A. Habib and T. Schenk, "A new approach for matching surfaces from laser scanners and optical sensors," in *International Archives of Photogrametry and Remote Sensing*, ser. Part 3 W14, vol. 32, 1999.

[7] S. Filin, "Recovery of systematic biases in laser altimeters using natural surfaces," in *International Archives of Photogrametry and Remote Sensing*, ser. Part 3 W3, vol. 34, 2001.

[8] S. M. Kay, *Fundamentals of Statistical Signal Processing: Estimation Theory*. Upper Saddle River, New Jersey: Prentice-Hall, Inc., 1993.

[9] D. P. Bertsekas, *Nonlinear Programming*, 2nd ed. Athena Scientific, 1999.

[10] J. Nocedal and S. Wright, *Numerical Optimization*, ser. Springer Series in Operation Reasearch. Springer, 1999.

[11] A. Edelman, T. A. Arias, and S. T. Smith, "Geometry of algorithms with orthogonality constraints," *SIAM Journal on Matrix Analysis and Aplications*, vol. 20, no. 2, pp. 303–353, 1998.

[12] P. A. Absil, R. Mahony, and R. Sepulchre, *Optimization Algorithms on Matrix Manifolds*. Princeton University Press, 2007.

[13] F. C. Park, J. Kim, and C. Kee, "Geometric descent algorithms for attitude determination using the global positioning system," *AIAA Journal of Guidance, Control and Dynamics*, vol. 23, no. 1, pp. 26–33, January-February 2000.

[14] M. Abramowitz and I. A. Stegun, *Handbook of Mathematical Functions with Formulas, Graphs, and Mathematical Tables*. New York: Dover Publications, 1972.